

# Three-body recombination with mixed sign light particles

**F Robicheaux**

Department of Physics, Auburn University, AL 36849-5311, USA

Received 25 September 2006

Published 3 January 2007

Online at [stacks.iop.org/JPhysB/40/271](http://stacks.iop.org/JPhysB/40/271)

## Abstract

Using a classical trajectory Monte Carlo method, we have computed the three-body recombination (two free positrons and an anti-proton scattering into one free positron and an anti-hydrogen atom:  $e^+ + e^+ + \bar{p} \rightarrow \bar{H} + e^+$ ) in the presence of electrons. By simply reversing the sign of all of the particles, these results can be applied to three-body recombination of matter in the presence of positrons. An important parameter is the fraction of light particles which are of the opposite sign; we performed calculations for several values of this parameter and find a substantial effect even for small fractions. We have also included a strong magnetic field in the calculation since this seems the most likely way to have mixed sign light particles in the same region of space. Our results will be useful for future anti-hydrogen experiments. We identify the main mechanisms controlling the recombination process.

## 1. Introduction

Recently, two groups [1, 2] reported the formation of anti-hydrogen ( $\bar{H}$ ) by having anti-protons ( $\bar{p}$ ) traverse a positron ( $e^+$ ) plasma. Presumably [3],  $\bar{H}$  is formed through the three-body recombination (TBR): two  $e^+$ 's scatter in the field of the  $\bar{p}$  so that one  $e^+$  loses enough energy to become bound to the  $\bar{p}$  and the other  $e^+$  carries away the excess energy. The theoretical treatment of this process is quite daunting due to the small cyclotron period of the  $e^+$ : 36 ps in a 1 T field. Compare this time scale with typical TBR rates for these experiments which have been roughly kHz; there are eight orders of magnitude between the two time scales.

TBR in a strong magnetic field was first treated in [4] where TBR in the  $B \rightarrow \infty$  limit was obtained. In this limit, the light particles are pinned to the field lines and the heavy particle is fixed in space. Later, [5] treated the large, but not infinite,  $B$  limit by allowing the light particles to have  $\vec{E} \times \vec{B}$  drift velocity for motion perpendicular to  $\vec{B}$  and allowing the heavy particle to have its full motion. The total rate was found to be approximately 60% larger than in the  $B \rightarrow \infty$  limit. More importantly, [5] reported that the TBR rate did not decrease rapidly with the velocity of the heavy particle suggesting the  $\bar{H}$ 's would form with energies much greater than  $k_B T$ . More detailed simulations [6] and measurements [7, 8] confirmed

that the majority of  $\bar{H}$  had kinetic energy substantially larger than  $k_B T$ . By launching the  $\bar{p}$  through the  $e^+$  plasma at lower energy, this problem can be averted. Reference [9] investigated the magnetic moment of  $\bar{H}$  formed in three-body recombination and found that only a small fraction of the  $\bar{H}$  could be trapped for the conditions in [6–8].

The high centre-of-mass energy of the  $\bar{H}$  formed by the original-mixing schemes has increased the relevance of other processes for the formation of  $\bar{H}$ . One possibility is the double charge exchange [10–12] first proposed in [10] and measured in [11]. In this process, a Rydberg atom is introduced into a positron plasma where a charge exchange makes Rydberg positronium which subsequently travels to a region of  $\bar{p}$ 's where a second charge exchange makes Rydberg  $\bar{H}$ . Since most of the centre-of-mass momentum of the  $\bar{H}$  is from the  $\bar{p}$ , the resulting  $\bar{H}$  will be cold if the original  $\bar{p}$  was at low temperature. Another possibility is to mix  $\bar{p}$ 's into a more diffuse  $e^+$  plasma and have the recombination occur by radiative processes which could, in principle, be enhanced by stimulated radiative recombination [13–15]. Because the TBR rate is proportional to the square of the  $e^+$  density while the slowing rate is proportional to the density, the diffuse  $e^+$  plasma will allow the  $\bar{p}$  to reach lower velocity before the recombination occurs.

Another possibility is to launch  $e^+$ 's through a plasma composed of  $\bar{p}$ 's and electrons. The electrons are present to keep the  $\bar{p}$ 's at a low temperature; the  $\bar{p}$ 's lose energy to the electrons through collisions and interactions with plasma waves. The electrons radiate this energy away due to their cyclotron motion. As with the previous two schemes, the resulting  $\bar{H}$  will have a lower centre-of-mass energy because the  $\bar{p}$  will start out cold. There are several possible processes that could lead to the formation of  $\bar{H}$ 's and their relative importance will depend on the temperature, and on the relative number and density of electrons,  $e^+$ 's, and  $\bar{p}$ 's. For example, there are two direct processes that could occur. When a  $e^+$  is passing by a  $\bar{p}$ , it can emit a photon and radiatively recombine. Or, if there is a high enough  $e^+$  density, there can be a three-body recombination. There are also indirect processes available. For example, a three-body recombination involving all light species (e.g., two  $e^+$  and an electron or two electrons and an  $e^+$ ) could give Rydberg positronium which then can give Rydberg  $\bar{H}$  through charge exchange with a  $\bar{p}$ . There could be even higher order indirect processes involving more than one charge transfer.

The indirect processes will depend strongly on the details of the plasmas (temperature, density, size and shape) and are, thus, of less general interest than the direct processes. In this paper, I examine the mechanisms that control the direct three-body recombination when both electrons and positrons are present. The recombination involves the competition between four basic processes. (1) The capture step which involves two  $e^+$ 's (or an electron and an  $e^+$ ) colliding in the field of the  $\bar{p}$  so that one of the  $e^+$ 's are captured. (2) Positron– $\bar{H}$  collisions cause the  $\bar{H}$  to change energy. When the binding energy of the  $\bar{H}$  is more than  $\sim 5k_B T$  the collisions mostly lead to an increase in binding energy (i.e., a decrease in principal quantum number  $\nu$ ). (3) Electron– $\bar{H}$  collisions cause the  $\bar{H}$  to change energy. As with positron collisions, the scattering mostly leads to a decrease in  $\nu$  when the binding energy is more than a few  $k_B T$ . (4) Electron– $\bar{H}$  collisions leading to charge transfer and the formation of Rydberg positronium. Clearly, processes (1)–(3) lead to a greater number and more deeply bound  $\bar{H}$ 's while process (4) destroys  $\bar{H}$ 's.

The different processes scale with different powers of the temperature and densities of the light species. In order to parameterize the effects of changing relative density, we will use  $n_e$  to be the sum of the densities of the electrons and positrons and use  $f$  to be the fraction of light particles that are electrons;  $T$  will be the temperature of the electrons and positrons which is assumed to be the same. The capture step (1) scales like  $T^{-9/2}$  and like  $n_e^2[(1-f)^2\gamma_1 + (1-f)f\gamma_2]$  where  $\gamma_1$  parameterizes the capture due to a pair of  $e^+$ 's and

$\gamma_2$  parameterizes the capture due to a  $e^+$  and an electron. The scaling of steps (2)–(4) is complicated by the magnetic field. Roughly, if the  $\bar{H}$  has an energy  $-13.6 \text{ eV}/v^2$ , then (2)–(4) scale like  $T^{1/2}$  and  $v^4$ . The dependence on density is that (2) scales like  $(1 - f)n_e$  while (3), (4) scale like  $fn_e$ .

There are several ways of shifting the balance of these different terms. In this paper, we vary the fraction,  $f$ , of electrons. We calculate the fraction of  $\bar{p}$ 's that have captured an  $e^+$  as a function of time and some of the properties of the resulting  $\bar{H}$ . We focus on the time dependence because the  $\bar{p}$ 's are only in the plasma for a limited time; thus, the evolution will be crucial for understanding experiments on this system. We restricted the simulations to times less than  $80 \mu\text{s}$ . This time corresponds to a  $\bar{p}$  travelling at  $125 \text{ m s}^{-1}$  ( $\sim 1 \text{ K}$ ) for a distance of  $1 \text{ cm}$ . Most  $\bar{p}$  will be in the plasma for much less time.

The calculations were performed for a large magnetic field:  $1 \text{ T}$ . The reason for this is two-fold. The next generation of  $\bar{H}$  experiments have recently begun and will involve magnetic fields of approximately this strength. Thus, the calculations will be directly relevant to this effort. Also, it seems likely that any future experiments that involve mixed sign light species will need to confine them by a magnetic field.

## 2. Numerical method

To simplify the discussion in this section, I will use the word lepton to refer to the light particle when it could be an electron or positron.

### 2.1. Approximations

The states formed by TBR in strong  $B$ -fields correspond to energies with principal quantum numbers greater than 30. The cyclotron motion is spread over several quantum states:  $k_B T / \hbar \omega_c \simeq 3$  where  $\omega_c$  is the cyclotron frequency. Thus, we can simulate TBR using classical equations of motion. For the leptons, we allowed them the full three-dimensional motion; we did not use the guiding centre approximation. The leptons are fired at the  $\bar{p}$  with the distribution described below. The coupled equations for the motion of the leptons are solved using an adaptive step size, Runge–Kutta method. This ODE solver does not conserve energy and the canonical angular momentum in the  $B$ -field direction, quantities conserved in the exact equations of motion. Thus, the numerical drift in these quantities are used as a gauge of the accuracy of a run. For example, the cumulative energy error during a run was required to be less than  $0.01 \text{ K}$ . Inevitably, some runs were rejected due to the too large drift in the conserved quantities. The number of rejected runs are too small to bias the results presented here.

The main approximation was treating the  $\bar{p}$  as being fixed in space, i.e. infinite mass. Because the mass of the  $\bar{p}$  is  $\sim 1840$  times larger than for the leptons, this seems a reasonable approximation. For the states of interest, all of the motions of the leptons have time scales over an order of magnitude shorter than those of the  $\bar{p}$ . This is another argument for treating the  $\bar{p}$  as stationary. Finally, we found that the three-body recombination rate in strong magnetic fields was unchanged within statistical uncertainty when the heavy particle was treated as fixed in space [9].

### 2.2. Initial distribution

The lepton distribution was similar to that described in [9] with the addition of a last random parameter that determined the sign of the charge. The distribution of trajectories is computed

using the physical distributions for the leptons. The leptons are randomly fired at a  $\bar{p}$  located at the centre of a cube. The time of firing a lepton is random with a probability  $\delta t/t_{\text{ave}}$  during the time interval  $\delta t$ ;  $t_{\text{ave}}$  is the average time a lepton takes to cross the volume. The cube has edges of length  $x_{\text{max}} = 10e^2/(4\pi\epsilon_0k_B T_e)$  which is  $\sim 100$  times larger than the radius of the recombined atom. The leptons are randomly fired from  $z = \pm x_{\text{max}}/2$  with the  $x, y$  position randomly chosen in the range  $-x_{\text{max}}/2 < x, y < x_{\text{max}}/2$ .<sup>1</sup> This prescription gives a varying number of leptons in the simulation. The leptons have a Maxwell–Boltzman distribution in  $\vec{v}$ . When a lepton is fired at the  $\bar{p}$ , the sign of its charge is determined by a last random number with a flat distribution between 0 and 1; when the random number is less than  $f$ , the lepton is an electron otherwise it is a positron.

In [5], we fired electrons until the binding energy was greater than a fixed multiple of the thermal energy. For the present simulation, this method is not practical due to the small time steps that are needed in the ODE solver to properly account for the cyclotron motion of the leptons. Instead we performed a two-step process similar in spirit to the method used in [4]; we used a similar method in [9].

The present calculations focus on the evolution of the fraction of  $\bar{p}$ 's that have captured an  $e^+$  and the properties of the resulting  $\bar{H}$ . In the first step, we generated a distribution of  $\bar{H}$  initial conditions by randomly firing leptons at the  $\bar{p}$  until only one  $e^+$  was inside the cube with an energy less than  $-k_B T$ . The time at which this occurred and the  $e^+$ 's position and velocity were stored. This was done for all of the different values of  $f$ , the fraction of electrons. There were approximately  $10^4$  examples from this step for each  $f$ . In the second stage, we performed roughly  $10^6$  runs with a duration of  $80 \mu\text{s}$ . For each run, we start at  $t = 0$  and randomly pick an  $\bar{H}$  from the first stage. The time,  $t$ , is incremented by a random amount given by the distribution of formation times from the first step. Next, we randomly fire leptons at it until the atom is ionized or  $80 \mu\text{s}$  is reached; during this step, the time is incremented normally. If the atom is ionized before  $80 \mu\text{s}$  is reached, another atom is randomly picked from the first step. The time,  $t$ , is incremented by a random amount given by the distribution of formation times from the first step, etc.

### 3. Results

In this section, we present the results of our calculations and simple models that reproduce the main features. All of the calculations were performed for a temperature of 4 K and a magnetic field of 1 T. The density of the leptons was such that on average only one lepton at a time was in a cube with edge length  $x_{\text{max}} = 10e^2/(4\pi\epsilon_0k_B T_e)$  which corresponds to a density of  $13.7 \times 10^6 \text{ cm}^{-3}$ .

#### 3.1. Capture rate

One of the interesting features of the calculation was the rate that  $\bar{H}$  formed with a binding energy of at least  $k_B T$ . This rate is *much* larger than the actual three-body recombination rate ( $\sim 200 \text{ Hz}$ ), because most of these atoms are reionized by  $e^+$ 's or electrons. To compute this rate, we fired leptons at the  $\bar{p}$  until only one  $e^+$  was in the cube and had an energy less than  $-k_B T$ . The average time that this occurred is the inverse of the capture rate. The last collision between the  $\bar{H}$  and the lepton that causes the binding energy to become larger than  $k_B T$  gives a distribution in energy that is peaked at  $-k_B T$  but has a long tail that extends to much deeper binding energy.

<sup>1</sup> We made sure the shape of the region was unimportant by comparing the results from calculations with different shape reaction region.

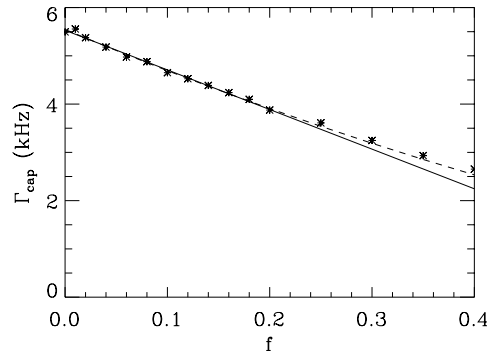


**Figure 1.** The positron capture rate into states with a binding energy greater than  $k_B T$ . The asterisks are the calculated data points whereas the two lines are fits as described in the text.

In figure 1, we show this rate versus the fraction,  $f$ , of leptons that were electrons. The calculation is shown as asterisks, and the lines are two different fits to the data. The rate decreases with increasing  $f$  because the TBR caused by the collision of two  $e^+$ 's is greater than that caused by the collision between an electron and a  $e^+$ ; also, there is the possibility for charge transfer destroying the  $\bar{H}$  which will decrease the formation rate. Because the binding energy is small for figure 1, we can think of the capture as if it were happening as a single step. The collision of two  $e^+$ 's is proportional to  $(1 - f)^2$  while the collision between an electron and positron is proportional to  $(1 - f)f$ . Thus, we might expect the capture rate to depend on  $f$  as  $(1 - f)^2 A + (1 - f)f B$  where  $A$  and  $B$  are constants.

The solid line is a linear fit to the data for  $f \leq 0.2$ :  $\Gamma_0 + f\Gamma_1$ ; the fit gives  $\Gamma_0 = 5526$  Hz and  $\Gamma_1 = -8208$  Hz. The dashed line is a fit to the data for  $f \leq 0.2$  using a form suggested by the physics:  $(1 - f)[(1 - f)\Gamma_{1s} + f\Gamma_{0s}]$ ; the fit gives  $\Gamma_{1s} = 5546$  Hz and  $\Gamma_{0s} = 2240$  Hz. The interpretation is  $\Gamma_{1s}$  characterizes the capture rate for a pair of  $e^+$ 's while  $\Gamma_{0s}$  characterizes the rate for an electron and  $e^+$ . The rate decreases approximately linearly over the range  $0 < f < 0.20$  and both fits give a good representation of the data. However, the linear fit clearly underestimates the rate for larger  $f$ . Also, the linear fit would give a rate of 0 for  $f = 5526/8208 \simeq 0.67$ . The physically motivated fit gives a rate of 0 for  $f = 1$  (no  $e^+$ ). Also, the parameters of the motivated fit are of a reasonable size with  $\Gamma_{1s}$  more than a factor of 2 larger than  $\Gamma_{0s}$ .

### 3.2. Time dependence of $\bar{H}$ population

We next turn our attention to the fraction of  $\bar{p}$  that have captured an  $e^+$  with a binding energy greater than  $4k_B T$ . This binding energy is deep enough that scattering by the leptons tends to drive the  $\bar{H}$  to more deeply bound states. However, charge transfer during a collision with an electron can still destroy the atom.

Figure 2 shows the time dependence of the probability,  $P(t)$ , a  $\bar{p}$  has become an  $\bar{H}$  with a binding energy greater than  $4k_B T$ . We plot data for  $f = 0.04, 0.08, 0.12, 0.16$  and  $0.20$ ; the data points are the symbols while the lines are the results from a simple model described below. There are several interesting features which can be understood qualitatively. For very early times,  $t < 5 \mu s$ , the probability is suppressed compared to extrapolations from later times. This is because the atoms cannot form instantaneously. Once an  $e^+$  is captured, many collisions with the leptons are needed to drive it to binding energies greater than  $4k_B T$ . This time delay is manifested as a suppression; the delay would be longer if we had chosen a deeper binding energy.

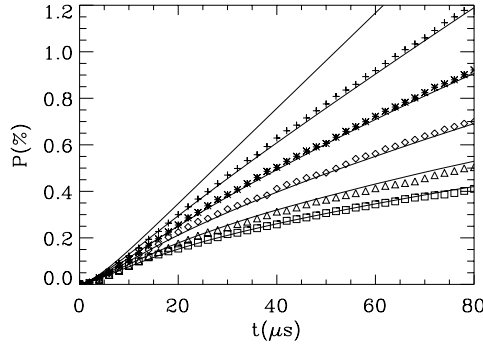


**Figure 2.** The population of  $\bar{p}$  that have captured a  $e^+$  with a binding energy greater than  $4k_B T$ . The symbols are the data points and the solid lines are the results from solving the simple rate equation described in the text. The uppermost line shows the population for  $f = 0$ : no electrons. The + are for  $f = 0.04$ , the \* are for  $f = 0.08$ , the diamonds are for  $f = 0.12$ , the triangles are for  $f = 0.16$  and the squares are for  $f = 0.20$ .

Another interesting feature is that the data do not lie on straight lines. This is important, because it appears that the population for  $f \sim 0.2$  are nearly reaching their steady state for *tiny* populations. For small probabilities (like those in figure 2), one expects a rate equation to give linear dependence:  $P(t) = 1 - \exp(-\Gamma t) \simeq \Gamma t$ . This time dependence arises from  $dP/dt = \Gamma \times (1 - P)$  (i.e., the rate of probability increase is  $\Gamma$  times the probability the  $\bar{H}$  has not formed). The definition of the TBR ‘rate’ becomes somewhat problematic because the  $P(t)$  is not a straight line, except for the smallest  $f$ ’s. Note that the bending is strongest for the largest  $f$ ’s. We have modelled this behaviour by assuming it arises from charge transfer. Qualitatively, the  $dP/dt$  has two terms. The first is from recombination and is positive while the second is from charge transfer and is negative.

We solved the equation

$$\frac{dP}{dt} = \Gamma_{\text{TBR}}^{(0)}(1 - f)^2[1 - P(t)] - \langle v^4 \rangle(t)\Gamma_{\text{ct},1}fP(t) \quad (1)$$

to produce the lines in figure 2. The first term in the right-hand side is the increase in population due to TBR where  $\Gamma_{\text{TBR}}^{(0)} = 205$  Hz is the  $f = 0$  TBR rate; this rate is computed from the expression in [5]. As discussed above, this is much smaller than the capture rates plotted in figure 1. Unlike the capture rate, we model the TBR rate as only arising from  $e^+e^-$  collisions; unlike the capture process, several collisions are needed to cause the  $\bar{H}$  to have a binding energy greater than  $4k_B T$  which will decrease the role of the electrons. The second term models the charge transfer rate. The parameter  $\Gamma_{\text{ct},1} = (2a_0)^2\sqrt{k_B T/mn_e}C$ , with  $C$  being a dimensionless constant, is the dimensional part of the charge transfer rate (see equation (1) of [12]) and  $\langle v^4 \rangle(t)$  is the average of  $v^4$  for atoms bound by more than  $4k_B T$ ; the radius of the atom is proportional to the square of the principal quantum number,  $\nu$ , so the cross section  $\sim \nu^4$ . The parameter  $\langle v^4 \rangle(t)$  decreases with  $t$  because scattering drives the atoms to more deeply bound states. In [12], we found that  $4 < C < 6.5$  depending on the temperature and magnetic field. The solid line results from solving the rate equation, equation (1), using the  $\langle v^4 \rangle(t)$  from our simulations. In our model, we used  $C = 4.25$  which is in the range from [12]. All of the curves are reproduced using only one adjustable parameter,  $C$ .

As a point of reference, the equation

$$\frac{dP}{dt} = \Gamma_1(1 - P) - \Gamma_2P \quad (2)$$

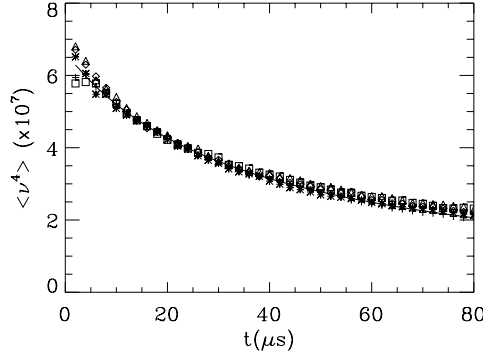


**Figure 3.** The average value of  $v^4$  for atoms bound by more than  $4k_B T$ . The symbols are the same as in figure 2. The solid line is from solving a simple rate equation as described in the text.

with  $P(0) = 0$  and constant  $\Gamma_1, \Gamma_2$  has the solution

$$P(t) = \frac{\Gamma_1}{\Gamma_1 + \Gamma_2} [1 - \exp(-(\Gamma_1 + \Gamma_2)t)]. \quad (3)$$

This result is interesting in that  $P(t) \rightarrow \Gamma_1/(\Gamma_1 + \Gamma_2) < 1$  as  $t \rightarrow \infty$  and that the time variation has the rate  $\Gamma_1 + \Gamma_2$ . The fact that  $P(t)$  is less than 1 for long time arises from the destruction by the process associated with the rate  $\Gamma_2$ . From above,  $\Gamma_1 = (1 - f)^2 \times 205$  Hz. To get the approximate size of  $\Gamma_2$ , we need  $\langle v^4 \rangle(t)$ . In figure 3, we plot this parameter for five different values of  $f$ . Remarkably, this parameter does not vary strongly with  $f$  compared to the dependence in figure 2. The  $\langle v^4 \rangle(t)$  decreases with time because the  $e^+$  scattering causes transitions to lower  $v$ . Before discussing the time dependence, we will use figure 3 to estimate  $\Gamma_2$ . For the estimate, we will use the smallest value  $2 \times 10^7$ ; note that the  $\langle v^4 \rangle^{1/4} \sim 65$  corresponds to a binding energy of  $\sim 35$  K. This gives  $\Gamma_2 = f \times 2.4 \times 10^4$  Hz.

For  $f = 0.2$ , the steady state population is  $\Gamma_1/(\Gamma_1 + \Gamma_2) \simeq 2.7\%$  and the total rate is  $\Gamma_1 + \Gamma_2 \sim 5$  kHz which is much faster than the TBR rate. For  $f = 0.1$ ,  $\Gamma_1/(\Gamma_1 + \Gamma_2) \simeq 6.5\%$  and  $\Gamma_1 + \Gamma_2 \sim 2.5$  kHz. Although the  $\langle v^4 \rangle(t)$  has time dependence so that the results of this paragraph are only qualitative, it is clear that even small fractions of electrons can strongly suppress the formation of  $\bar{H}$ .

As a final point, the curve on figure 3 results from a very simple model. The average

$$\langle v^4 \rangle = \frac{1}{N} \sum_j \left( \frac{13.6 \text{ eV}}{E_j} \right)^2, \quad (4)$$

where the  $E_j$  is the energy of the  $j$  th  $\bar{H}$ ,  $N$  is the number of atoms with a binding energy greater than  $4k_B T$ , and the sum is only over atoms with a binding energy greater than  $4k_B T$ . The time derivative is

$$\frac{d}{dt} \langle v^4 \rangle \propto \sum_j \frac{1}{E_j^3} \frac{dE_j}{dt} \propto \sum_j v_j^6 v_j^4 (A \times E_j) \propto - \sum_j v_j^8, \quad (5)$$

where  $dE/dt$  has been approximated as being proportional to the geometric cross section of the atom,  $v^4$ , times an energy change proportional to the energy. For early times,  $\langle v^8 \rangle \sim \langle v^4 \rangle^2$ . Thus we arrive at a differential equation that has the form  $dx/dt \propto -x^2$  which has the solution  $x(t) = B/(t + t_0)$  where  $B$  and  $t_0$  are constants. The solid line in figure 3 is  $6.64 \times 10^7 / (1 + [t/36 \mu\text{s}])$ . The time scale  $36 \mu\text{s}$  corresponds to a rate of 28 kHz which should be compared to the scattering time scale, 24 kHz, in the  $\Gamma_2$  above. We note that the curves

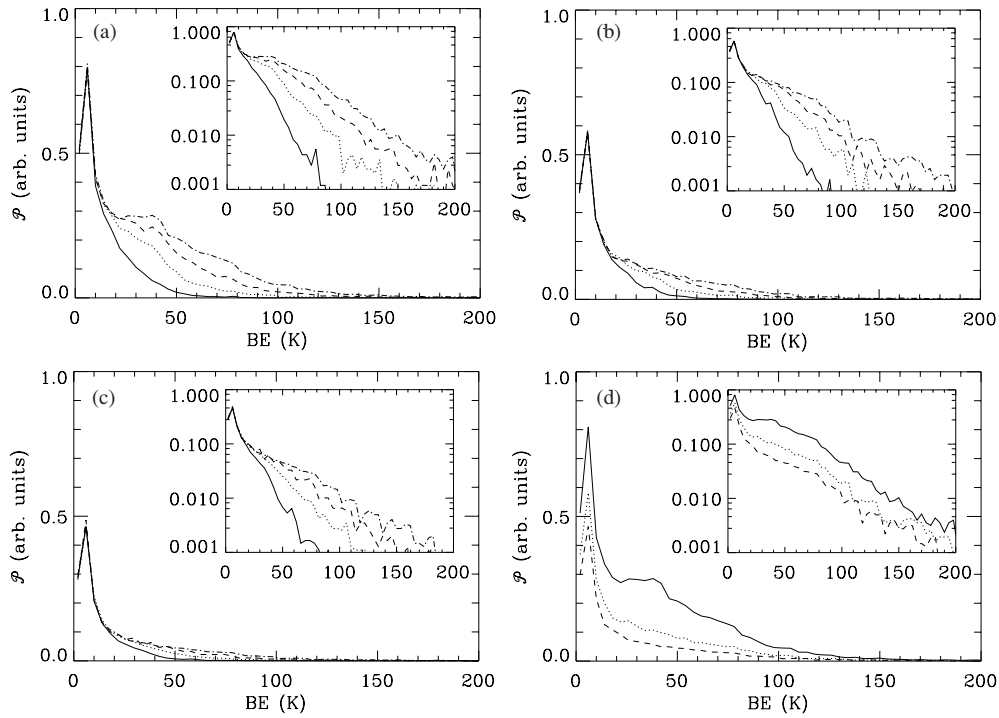


**Figure 4.** The energy distribution of  $\bar{H}$  as a function of time for (a)  $f = 0.01$ , (b)  $f = 0.12$ , and (c)  $f = 0.20$ . All data sets have been converted to the same  $y$ -scale so that overall height reflects the total number of  $\bar{H}$  atoms. In these three figures, the solid line is at  $20 \mu\text{s}$ , the dotted line is at  $40 \mu\text{s}$ , the dashed line is at  $60 \mu\text{s}$ , and the dash-dot line is at  $80 \mu\text{s}$ . The inset is the same data but on a log-scale for the  $y$ -axis. Figure (d) compares the  $80 \mu\text{s}$  data for  $f = 0.01$  (solid line),  $f = 0.12$  (dotted line), and  $f = 0.20$  (dashed line).

in figure 3 are quite simple so other forms fit the data equally well (e.g.  $A + B \exp(-\Gamma t)$  with  $A$ ,  $B$ , and  $\Gamma$  constants). Finally, the trend at later times is for  $\langle v^4 \rangle^2$  to be *larger* for larger  $f$ . This is because the charge transfer destroys the atom before it can be scattered into more deeply bound states with smaller  $v$ . This will be seen more clearly in the next section.

### 3.3. Energy distributions

One of the main questions that can be answered is what type of atom is formed in TBR. We recently found [9] that the distribution of magnetic moments is not random when  $\bar{H}$  is formed by TBR in a strong magnetic field. Most importantly we found that the atoms tend to be attracted to high fields which cannot be trapped using multipole magnetic fields. As the binding energy of the atoms increase, the magnetic moments become more random and there is an increased chance that the atom can be trapped.

In figure 4, we plot the energy distribution at  $20$ ,  $40$ ,  $60$  and  $80 \mu\text{s}$  for  $f = 0.01$ ,  $0.12$  and  $0.20$ . We also plot the distribution for  $f = 0.01$ ,  $0.12$  and  $0.20$  at  $80 \mu\text{s}$ . The case  $f = 0.01$  is hardly different from  $f = 0$  over this time range. All three values of  $f$  have a similar type of time behaviour. At early  $t$ , the distribution does not extend to deep binding. This is because the atoms reach these energies through scattering and there has not been enough scattering events to reach these binding energies. At later times, the distribution for weak binding does not change very much. This is because TBR starts from weak binding and this region reaches



a steady state value most rapidly. It is interesting that the  $f = 0.2$  seems to have reached steady state down to  $\sim 50$  K whereas the  $f = 0.01$  is in steady state only down to  $\sim 25$  K.

The  $f = 0.01$  and  $f = 0.2$  develop in a quantitatively different manner. A minimum appears to be developing near 25 K for  $f = 0.01$  whereas the  $f = 0.2$  monotonically decreases from  $\sim 4$  K. For  $f = 0.01$ , there is little charge transfer so the distribution develops similar to  $f = 0$ . The minimum is the bottleneck for TBR. The largest relative difference between  $f = 0.01$  and  $f = 0.2$  occurs for  $\sim 40$  K. This is because the more deeply bound atoms arise from one or a few lucky collisions that remove substantial energy. Because these atoms are physically much smaller, there is less chance for a charge transfer. The atoms with binding  $\sim 40$  K arise from many small energy changing collisions. Because they are physically large, the chance for charge transfer destroying them is great. The differences become more accentuated for longer times than those shown here. If, by chance, an atom were to be in the plasma for 200  $\mu\text{s}$ , the  $f = 0.01$  distribution would give a substantial number of atoms with binding energies greater than 100 K, but the  $f = 0.2$  distribution would not greatly increase in that range.

#### 4. Conclusions

We have performed calculations of the formation of  $\bar{\text{H}}$  through three-body recombination (TBR) when both electrons and positrons are present. The calculations use classical trajectory Monte Carlo methods to obtain results for several values of the fraction of electrons. The calculations do not use the guiding centre approximation. We have also developed simple models that adequately describe the main results.

Most importantly, we found that even a small fraction of electrons reduce the recombination by large amounts. For example, the maximum fraction of  $\bar{\text{p}}$  that can form  $\bar{\text{H}}$  decreases to just a couple per cent when the density of electrons is only 1/4 that of the positrons. Another important point is that the electrons prevent the  $\bar{\text{H}}$  population from developing deeply bound states. This is of crucial importance because the weakly bound atoms are more likely to be attracted to high magnetic fields [9]; atoms attracted to high magnetic fields cannot be trapped. The few deeply bound  $\bar{\text{H}}$  are formed through a couple of lucky collisions that remove substantial energy.

Our results show the necessity for reducing the fraction of electrons to the smallest possible number if TBR is the mechanism used in forming  $\bar{\text{H}}$ . If a different mechanism is used, then the conclusions might change. For example, the electrons might not have a substantial effect on atoms formed by radiative recombination because they are typically formed in deeply bound states.

#### Acknowledgments

This work was supported by the Chemical Sciences, Geosciences and Biosciences Division of the Office of Basic Energy Sciences, US Department of Energy and by the Office of Fusion Energy, US Department of Energy. This research was performed in part using the Molecular Science Computing Facility (MSCF) in the William R Wiley Environmental Molecular Sciences Laboratory, a national scientific user facility sponsored by the US Department of Energy's Office of Biological and Environmental Research and located at the Pacific Northwest National Laboratory, operated for the Department of Energy by Battelle.

#### References

- [1] Amoretti M *et al* (ATHENA Collaboration) 2002 *Nature* **419** 456
- [2] Gabrielse G *et al* (ATRAP Collaboration) 2002 *Phys. Rev. Lett.* **89** 213401

- 
- [3] Gabrielse G *et al* 1988 *Phys. Lett. A* **129** 38
  - [4] Glinsky M E and O'Neil T M 1991 *Phys. Fluids B* **3** 1279
  - [5] Robicheaux F and Hanson J D 2004 *Phys. Rev. A* **69** 010701
  - [6] Robicheaux F 2004 *Phys. Rev. A* **70** 022510
  - [7] Gabrielse G *et al* (ATRAP Collaboration) 2004 *Phys. Rev. Lett.* **93** 073401
  - [8] Madsen N *et al* (ATHENA Collaboration) 2005 *Phys. Rev. Lett.* **94** 033403
  - [9] Robicheaux F 2006 *Phys. Rev. A* **73** 033401
  - [10] Hessels E A, Homan D M and Cavagnero M J 1998 *Phys. Rev. A* **57** 1668
  - [11] Storry C H *et al* 2004 *Phys. Rev. Lett.* **93** 263401
  - [12] Wall M L, Norton C S and Robicheaux F 2005 *Phys. Rev. A* **72** 052702
  - [13] Fill E E 1986 *Phys. Rev. Lett.* **56** 1687
  - [14] Schramm U *et al* 1991 *Phys. Rev. Lett.* **67** 22
  - [15] Yousif F B *et al* 1991 *Phys. Rev. Lett.* **67** 26
  - [16] Mansbach P and Keck J 1969 *Phys. Rev.* **181** 275